脂多糖受体 CD14 在急性脑出血应激性肝损害中的作用及星蒌承气汤的效应研究

Role of CD14 in hepatic stress injury of acute cerebral hemorrhage and effect of Xinglou Chengqi Tang

（正文见第 21 页　Refer to P21）

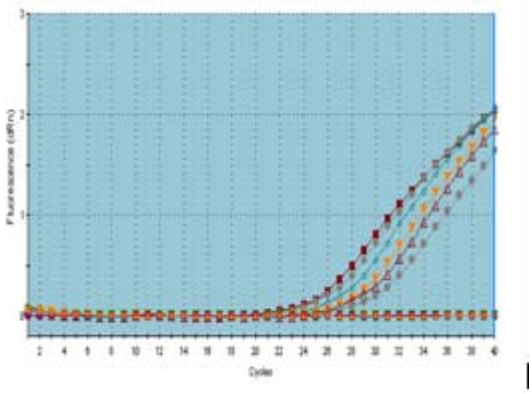

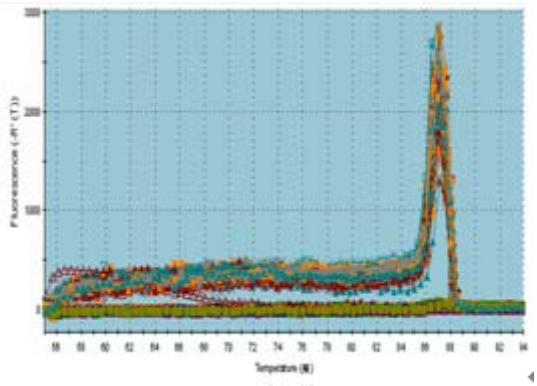

注：纵坐标为荧光信号量，横坐标为 PCR 反映循环数。

Note: Ordinateis fluorescent signal, abscissaiscycle number reflected by PCR.

图 1　大鼠肝 CD14mRNA 扩增曲线图　　图 2　大鼠肝 CD14 溶解曲线图

Fig.1　CD14 mRNA amplification curve of rat liver　Fig.2　CD14 mRNA dissolution curve of rat liver

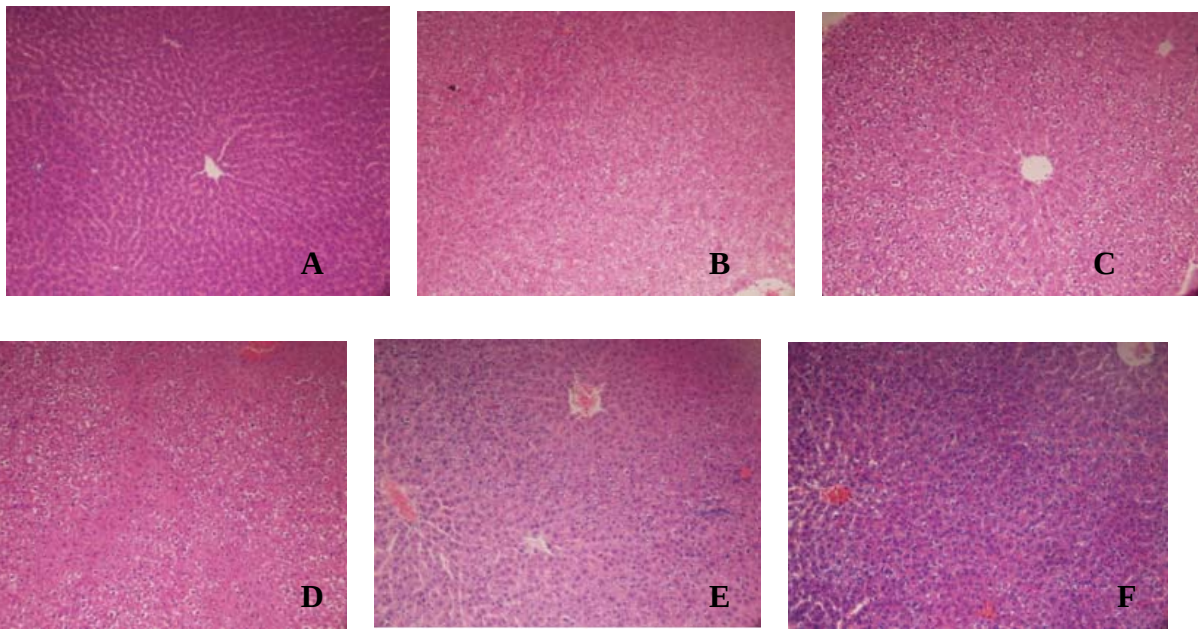

A 正常组；B 24 h 脑出血痰热腑实证组；C 48 h 脑出血痰热腑实证组；D 72 h 脑出血痰热腑实证组；E　48 h 星蒌承气汤组；F 72 h 星蒌承气汤组。

A normal group; B 24-h group of phlegm-heat and bowel-excess syndrome; C 48-h group of phlegm-heat and bowel-excess syndrome; D 72-h group of phlegm-heat and bowel-excess syndrome; E 48-h Xonglou Chengqi Tang group; F 72-h Xonglou Chengqi Tang group.

图 3　大鼠肝脏病理形态改变　（HE×20）

Fig. 3　Pathomorphological changes of rat liver (HE　×20)

眼针对大鼠急性脑缺血再灌注损伤脑组织 ICAM–1 表达的影响

Influence of eye acupuncture on expression of brain ICAM–1 in rats with acute cerebral ischemia and reperfusion injury

（正文见第 39 页 refer to P39）

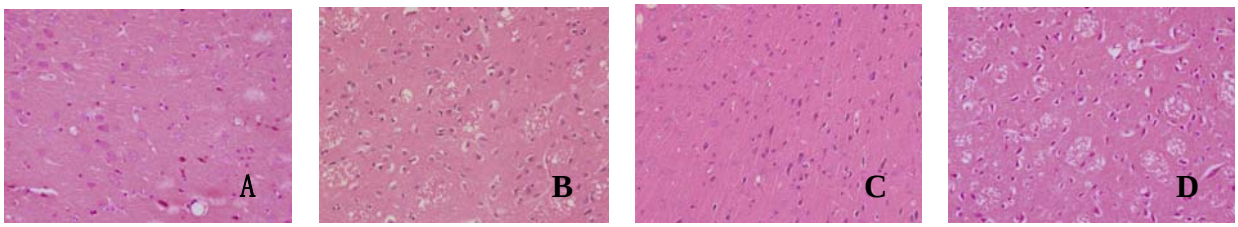

A 空白对照组；B 眼针组；C 假手术组；D 模型组。

A blank group; B eye acupuncture group; C sham-operation group; D model group.

图 1　各组大鼠脑组织病理变化（HE×400）

Fig. 1　Pathological changes of brain in rats of all groups (HE　×400)

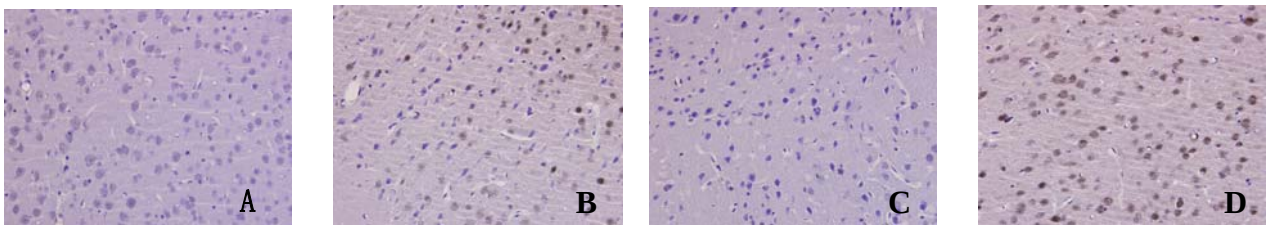

A 空白对照组；B 眼针组；C 假手术组；D 模型组。

A blank group; B eye acupuncture group; C sham-operation group; D model group.

图 2　各组大鼠脑组织 ICAM-1 免疫组化实验结果（DAB×400）

Fig. 2　Immunohistochemistry results of brain ICAM-1 in rats of all groups (DAB　×400)

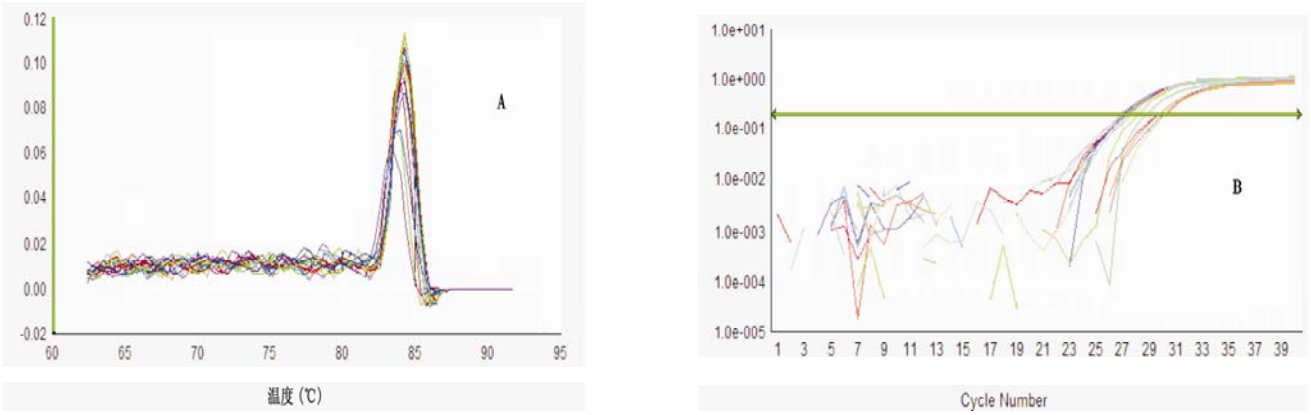

A ICAM-1 mRNA 溶解曲线；B ICAM-1mRNA 扩增曲线。

A dissolution curve of ICAM-1mRNA; B amplification curve of ICAM-1mRNA.

图 4　各组大鼠脑组织中 ICAM-1 mRNA 表达实时定量 PCR 结果

Fig. 4　Results of RT-PCR of brain ICAM-1 expression in rats of all groups

证候热力学研究初探
Syndrome thermodynamics research

（正文见第 43 页　refer to P43）

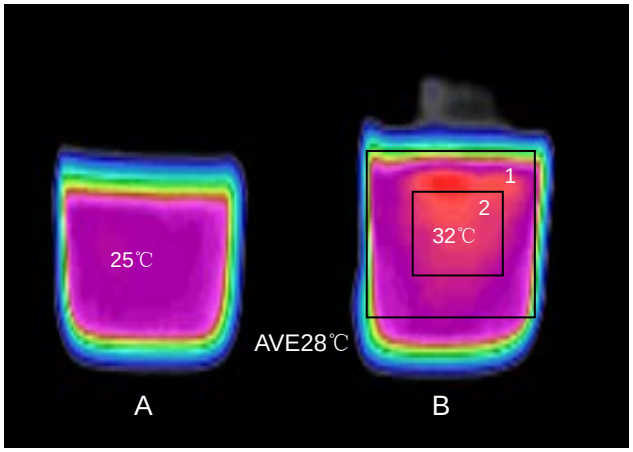

A 对照容器；B 耗散结构；1 阳区，温度较高的区域；
2 阴区，温度较低的区域。

A Reference sample; B Dissipative structure;
1 Yang region; 2 Yin region.

图 1 耗散结构红外成像热图及阳区阴区划分

Fig. 1 Dissipative structure infrared thermal-imaging and partition of yang and yin regions

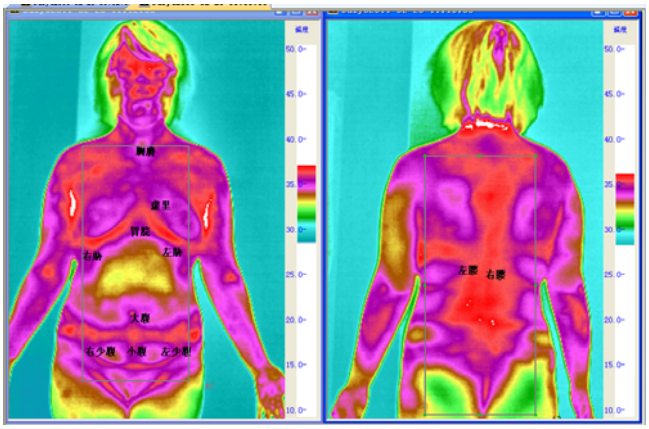

图 2 人体红外成像区域划分图

Fig. 2 Regional division of human body infrared imaging

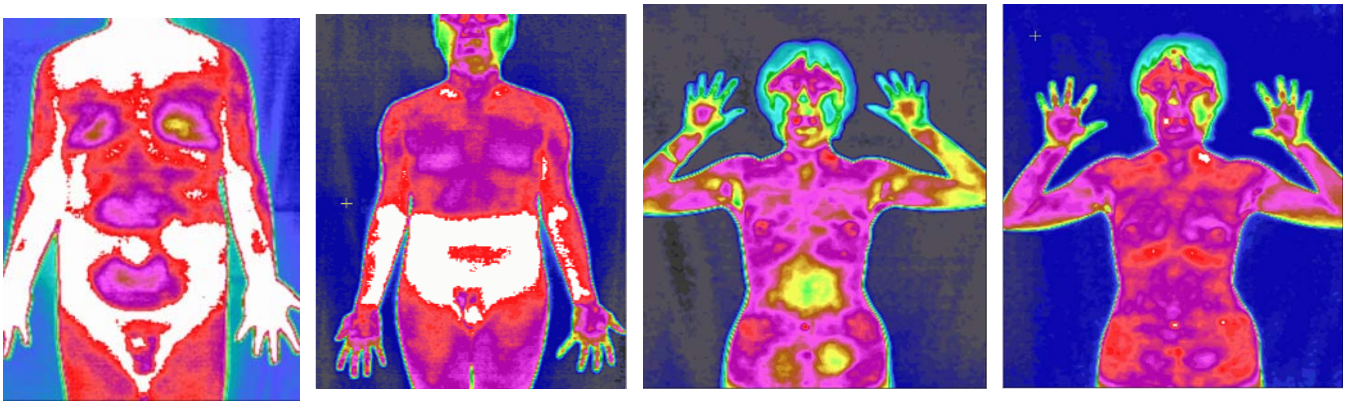

A 阳明腑实证，下焦△T:2.5℃；B 心阳虚证，虚里△T：-2.5℃；C 胆郁痰扰证治疗前，△T:-1.6℃；D 胆郁痰扰证治疗后，△T:-0.8℃。

A Yangming bowel excess syndrome, lower energizer △T: 2.5; B heart-yang deficiency syndrome, heart apex △T: -2.5; C depressed gallbladder with harassing phlegm syndrome before treatment, △T: -1.6℃; D depressed gallbladder with harassing phlegm syndrome before treatment, △T: -0.8℃

图 6 不同证型红外热图

Fig. 6 Infrared thermal-imaging of different syndrome types

电针肝俞、期门对肝气郁结模型大鼠正电子发射脑功能成像研究

（正文见第 页 refer to P ）

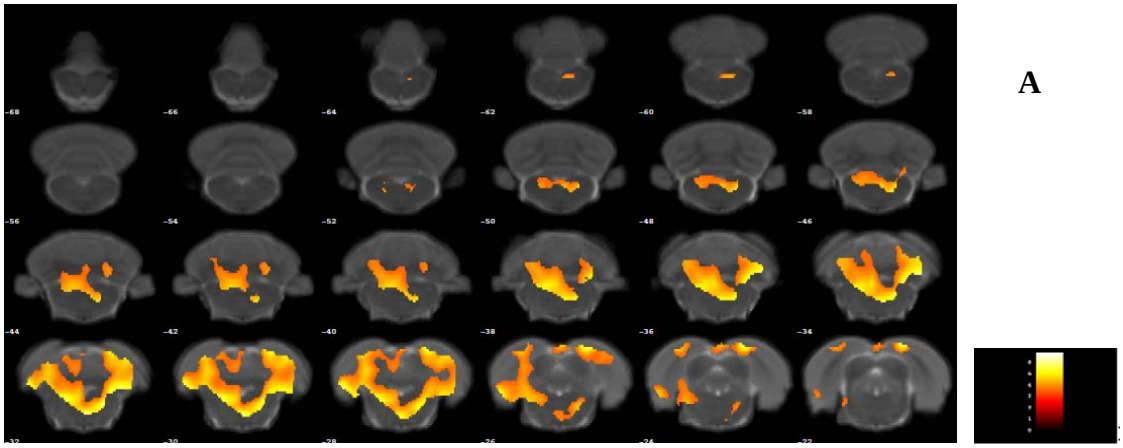

A

左 left　　右 right

注：A 代谢减低区激活图；B 代谢增高脑区激活图，染色区域为葡萄糖代谢增高脑区；右下角图示代表激活由强到弱的变化（由黄色到红色递减）。

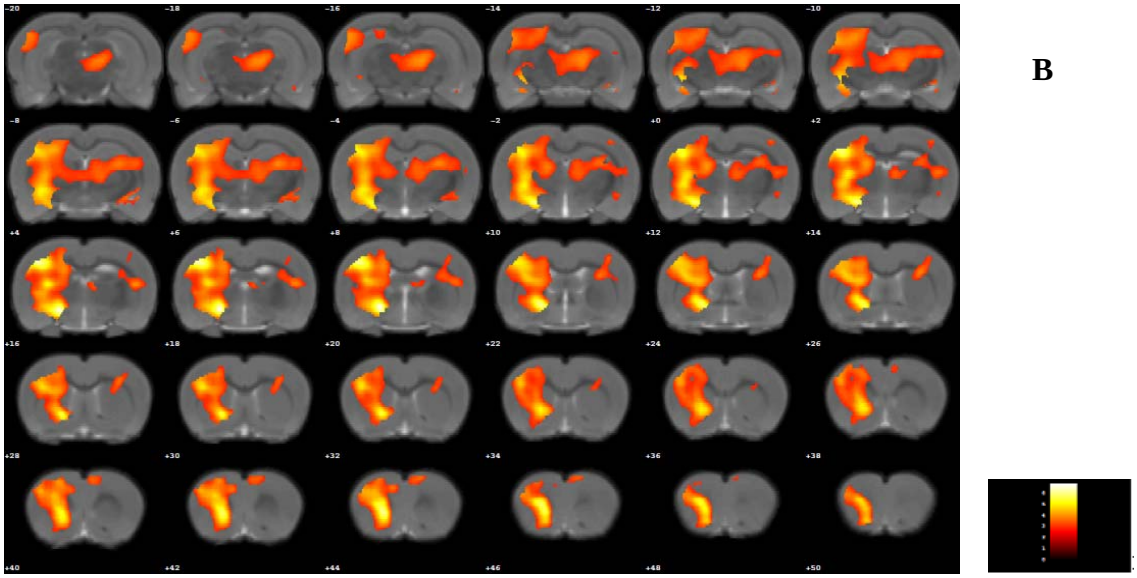

B

左 left　　右 right

注：染色区域为葡萄糖代谢增高脑区。右下角图示代表激活由强到弱的变化（由黄色到红色递减）。

Staining region is the brain areas with increased glucose metabolism. Icon of activation in the right corner indicates the change from strong to weak (decreasing from yellow to red)

图 1　电针组大鼠较模型组葡萄糖代谢变化脑区激活图（冠状图）

Fig.1　The brain areas of EA group rats with increased glucose metabolism compared with model group (corona- figure)